

Non-Darcy Natural Convection from a Vertical Wavy Surface in a Porous Medium

D. A. S. REES¹ and I. POP²

¹*School of Mechanical Engineering, University of Bath, Claverton Down, Bath BA2 7AY, U.K.*

²*Faculty of Mathematics, University of Cluj, R-3400, Cluj, CP 253, Romania*

(Received: 9 June 1994; in final form: 7 September 1994)

Abstract. We examine the combined effect of spatially stationary surface waves and the presence of fluid inertia on the free convection induced by a vertical heated surface embedded in a fluid-saturated porous medium. We consider the boundary-layer regime where the Darcy–Rayleigh number, Ra , is very large, and assume that the surface waves have $O(1)$ amplitude and wavelength. The resulting boundary-layer equations are found to be nonsimilar only when the surface is nonuniform and inertia effects are present; self-similarity results when either or both effects are absent. Detailed results for the local and global rates of heat transfer are presented for a range of values of the inertia parameter and the surface wave amplitude.

Key words: Porous medium, convection, boundary layer, nonsimilarity, inertia, surface waves.

Nomenclature

a	amplitude of the wavy surface.
d	particle diameter.
f	reduced streamfunction.
g	acceleration due to gravity.
Gr^*	modified Gashof number.
k_c	effective thermal conductivity.
K	permeability.
\tilde{K}	material parameter.
l	half-wavelength, or lengthscale associated with the surface.
\mathcal{L}^2	differential operator; see Equation (17).
\mathbf{n}	unit vector normal to the wavy surface.
Nu	local Nusselt number.
p	pressure.
q	rate of heat flux.
Q	nondimensional velocity; see Equation (11).
Ra	Darcy–Rayleigh number based on l .
s	surface length.
T	temperature.
u, v	fluid velocities in the x and y directions, respectively.
\mathbf{v}	velocity vector.
x, y	streamwise and cross-stream Cartesian coordinates.

Greek Symbols

α	thermal diffusivity of the porous medium.
β	coefficient of thermal expansion.
ϵ	porosity.
ξ, η	pseudo-similarity variables.
σ	surface profile; see Equation (1).
θ	dimensionless temperature.
μ	dynamic viscosity.
ν	kinematic viscosity.
ρ	density
ψ	streamfunction.

Superscripts

$^-$	dimensional variables.
\sim	transformed variables ($\xi < 1$).
$\hat{}$	boundary-layer variables.
$'$	differentiation with respect to η .

Subscripts

g	global.
x	differentiation with respect to x .
w	condition at the wall.
∞	condition at infinity.

1. Introduction

Natural convection within fluid-saturated porous media has attracted considerable attention in the last three decades because of its importance in geophysics, oil recovery techniques, thermal insulation engineering, packed-bed catalytic reactors, and heat storage beds. In many practical situations surfaces are intentionally roughened in order to enhance the rate of heat transfer. The presence of roughened surface alters the flowfield and alters the heat transfer characteristics. Larger scale nonuniformities are sometimes encountered in grain-storage containers where walls are buckled, and in cavity-wall insulating systems.

A number of similarity solutions and numerical studies of natural convection in porous media have been presented. A comprehensive survey of relevant papers may be found in the recent monograph by Nield and Bejan [1]. Most of the studies included there refer to bodies of relatively simple geometry, such as flat plates, cylinders and spheres. However, natural convection from bodies of more complicated geometries embedded in a porous medium has not received very great attention to date. An elegant general transformation has been proposed recently by Nakayama and Koyama [2,3] to study the problem of natural convection from a two-dimensional or axisymmetric body of otherwise arbitrary geometrical configuration. Recently, some studies have been carried out by Rees and Pop [4-6] to

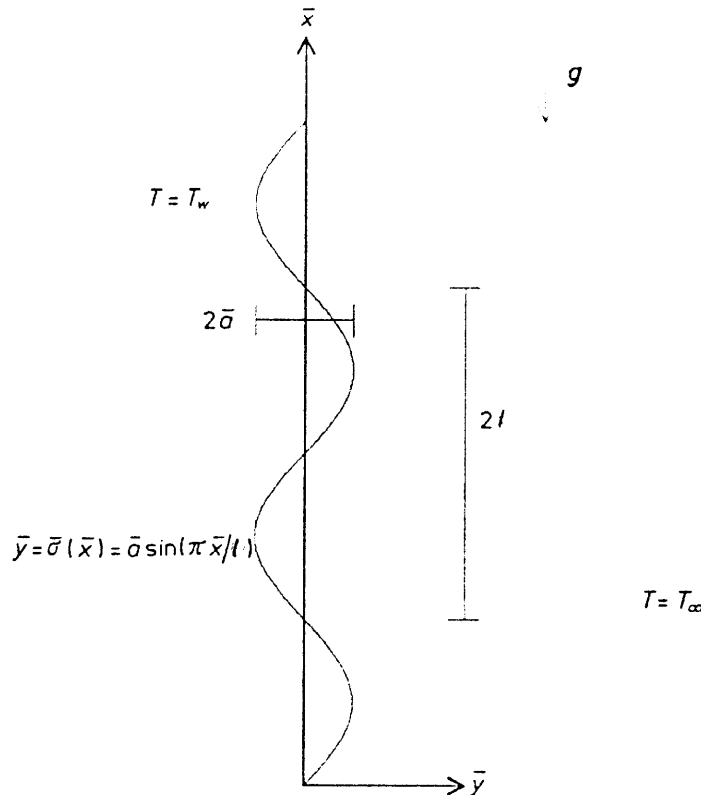


Fig. 1. Physical model and coordinate system depicting transverse surface waves.

analyse natural convection from vertical and horizontal wavy surfaces embedded in a porous medium under the assumption of the Darcy law model. This model, however, is known to be valid only for relatively slow flows through the porous matrix. In general, we must consider the effect of the fluid inertia, as well as viscous diffusion which may well become significant for materials with very high porosities such as fibrous and foams.

In this paper, we consider the combined effect of fluid inertia and steady surface waves on one of the most fundamental natural convection problems, namely, the steady thermal boundary-layer flow induced by a uniformly heated vertical surface. In order to account for the inertia effects, the nonlinear Ergun [7] model will be considered. The same model was employed by Plumb and Huenefeld [8], Vasantha *et al.* [9], Lai and Kulacki [10], Riley and Rees [11] and Nakayama *et al.* [12]. It will be shown that the governing boundary-layer equations are nonsimilar, unlike the corresponding plane-wall Darcy case, and the Keller-box method is employed to solve the governing equations. Numerical results are presented for a selection of parameter sets consisting of the surface wave amplitude and a nondimensional number which measures the strength of the fluid inertia. Heat transfer characteristics are discussed in detail.

2. Governing Equations

We consider a vertical surface which exhibits steady transfer waves of amplitude, \bar{a} , and wavelength, $2l$, and which is embedded in a homogeneous fluid-saturated

porous medium, as shown in Figure 1. In particular, we assume that the surface profile is given by

$$\bar{y} = \bar{\sigma} = \bar{a} \sin(\pi \bar{x}/l). \quad (1)$$

The surface is held at the constant temperature, T_w , whilst the ambient temperature of the medium is T_∞ . We assume that $T_w > T_\infty$ and examine the resulting two-dimensional flow induced by buoyancy forces in the medium along the wavy surface. We take as our constitutive equation,

$$-\frac{K}{\mu} [\nabla p + \rho \mathbf{g}] = \left[1 + \frac{\tilde{K}}{\mu} \rho |\mathbf{v}| \right] \mathbf{v}, \quad (2)$$

(see Riley and Rees [11]) where Darcy's law is recovered when $\tilde{K} = 0$. Here, K is the permeability of the porous medium and \tilde{K} is a material parameter which may be thought of as a measure of the inertial impedance of the matrix. $\mathbf{v} = (\bar{u}, \bar{v})$ is the velocity flux vector, \mathbf{g} the acceleration due to gravity, ρ the fluid density, and μ the dynamic viscosity. To illustrate how the additional nonlinear term comes into play when the porosity is high we quote Ergun's relations for K and \tilde{K} ,

$$K = \frac{d^2 \epsilon^3}{150(1 - \epsilon)^2}, \quad \tilde{K} = \frac{1.75d}{150(1 - \epsilon)}, \quad (3)$$

(see [7]) where ϵ denotes the porosity, and d is the characteristic pore or particle diameter. Clearly, when $(\tilde{K}/\mu)\rho|\mathbf{v}|$ is near to or greater than 1 at any point in the flowfield the nonlinear term is important.

On assuming that the Boussinesq approximation is valid, the governing equations for the present problem become

$$\frac{\partial \bar{u}}{\partial \bar{x}} + \frac{\partial \bar{v}}{\partial \bar{y}} = 0, \quad (4)$$

$$\frac{K}{\mu} \left[-\frac{\partial \bar{p}}{\partial \bar{x}} + \rho g \beta (T - T_\infty) \right] = \left[1 + \frac{\tilde{K}}{\mu} \rho |\mathbf{v}| \right] \bar{u}, \quad (5)$$

$$-\frac{K}{\mu} \frac{\partial \bar{p}}{\partial \bar{y}} = \left[1 + \frac{\tilde{K}}{\mu} \rho |\mathbf{v}| \right] \bar{v}, \quad (6)$$

$$\bar{u} \frac{\partial T}{\partial \bar{x}} + \bar{v} \frac{\partial T}{\partial \bar{y}} = \alpha \left[\frac{\partial^2 T}{\partial \bar{x}^2} + \frac{\partial^2 T}{\partial \bar{y}^2} \right], \quad (7)$$

where (\bar{u}, \bar{v}) are the velocity components along the (\bar{x}, \bar{y}) -axes, T is the temperature, β is the thermal expansion coefficient, and α is the thermal diffusivity of the saturated porous medium.

On introducing the nondimensional variables,

$$(x, y) = (\bar{x}, \bar{y})/l, \quad \theta = \frac{T - T_\infty}{T_w - T_\infty}, \quad a = \bar{a}/l, \\ \sigma(x) = \bar{\sigma}(\bar{x})/l, \quad (8a)$$

and a nondimensional streamfunction, ψ , such that

$$\left(\frac{\partial \psi}{\partial y}, -\frac{\partial \psi}{\partial x} \right) = \frac{\nu}{gK\beta(T_w - T_\infty)} (\bar{u}, \bar{v}), \quad (8b)$$

we obtain, after eliminating the pressure,

$$(1 + \text{Gr}^* Q) \nabla^2 \psi + \\ + \frac{\text{Gr}}{Q} \left[\left(\frac{\partial \psi}{\partial x} \right)^2 \frac{\partial^2 \psi}{\partial x^2} + 2 \frac{\partial \psi}{\partial x} \frac{\partial \psi}{\partial y} \frac{\partial^2 \psi}{\partial x \partial y} + \left(\frac{\partial \psi}{\partial y} \right)^2 \frac{\partial^2 \psi}{\partial y^2} \right] = \frac{\partial \theta}{\partial y}, \quad (9)$$

$$\nabla^2 \theta = \text{Ra} \left(\frac{\partial \psi}{\partial y} \frac{\partial \theta}{\partial x} - \frac{\partial \psi}{\partial x} \frac{\partial \theta}{\partial y} \right). \quad (10)$$

Here, ∇^2 is the two-dimensional Laplacian operator, $\text{Gr}^* = gK\tilde{K}\beta(T_w - T_\infty)/\nu^2$ is a modified Grashof number expressing the relative importance of inertia effects and viscous effects, $\text{Ra} = gK\beta(T_w - T_\infty)l/\alpha\nu$ is the Darcy–Reyleigh number, and Q is a nondimensional velocity given by

$$Q = \left[\left(\frac{\partial \psi}{\partial x} \right)^2 + \left(\frac{\partial \psi}{\partial y} \right)^2 \right]^{1/2}. \quad (11)$$

When $\text{Gr}^* = 0$ inertial effects are absent, and buoyancy forces are balanced solely by viscous effects; that is, we recover Darcy's law. The associated boundary conditions are

$$\psi = 0, \quad \theta = 1 \quad \text{on} \quad y = \sigma(x) = a \sin(\pi x), \quad (12a)$$

$$\frac{\partial \psi}{\partial y} \rightarrow 0, \quad \theta \rightarrow 0 \quad \text{as} \quad y \rightarrow \infty. \quad (12b)$$

The effect of the wavy surface can be transferred from the boundary conditions into the governing equations by means of the coordinate transformation given by

$$\tilde{x} = x, \quad \tilde{y} = y - \sigma(x). \quad (13)$$

Equations (9) and (10) now become

$$\begin{aligned} & (1 + \text{Gr}^* Q) \mathcal{L}^2 \psi + \\ & + \frac{\text{Gr}^*}{Q} \left\{ \left(\frac{\partial \psi}{\partial \tilde{x}} - \sigma_{\tilde{x}} \frac{\partial \psi}{\partial \tilde{y}} \right)^2 \left[\frac{\partial^2 \psi}{\partial \tilde{x}^2} - 2\sigma_{\tilde{x}} \frac{\partial^2 \psi}{\partial \tilde{x} \partial \tilde{y}} - \sigma_{\tilde{x} \tilde{x}} \frac{\partial \psi}{\partial \tilde{y}} + \sigma_{\tilde{x}}^2 \frac{\partial^2 \psi}{\partial \tilde{y}^2} \right] + \right. \\ & \left. + 2 \frac{\partial \psi}{\partial \tilde{y}} \left(\frac{\partial \psi}{\partial \tilde{x}} - \sigma_{\tilde{x}} \frac{\partial \psi}{\partial \tilde{y}} \right) \left(\frac{\partial^2 \psi}{\partial \tilde{x} \partial \tilde{y}} - \sigma_{\tilde{x}} \frac{\partial^2 \psi}{\partial \tilde{y}^2} \right) + \left(\frac{\partial \psi}{\partial \tilde{y}} \right)^2 \frac{\partial^2 \psi}{\partial \tilde{y}^2} \right\} \\ & = \frac{\partial \theta}{\partial \tilde{y}}, \end{aligned} \quad (14)$$

$$\mathcal{L}^2 \theta = \text{Ra} \left(\frac{\partial \psi}{\partial \tilde{y}} \frac{\partial \theta}{\partial \tilde{x}} - \frac{\partial \psi}{\partial \tilde{x}} \frac{\partial \theta}{\partial \tilde{y}} \right), \quad (15)$$

and the boundary conditions (12) become

$$\psi = 0, \quad \theta = 1 \quad \text{on} \quad \tilde{y} = 0, \quad (16a)$$

$$\frac{\partial \psi}{\partial \tilde{y}} \rightarrow 0, \quad \theta \rightarrow 0 \quad \text{as} \quad \tilde{y} \rightarrow \infty. \quad (16b)$$

In Equations (14) and (15) the operator \mathcal{L}^2 is defined as follows,

$$\mathcal{L}^2 = (1 + \sigma_{\tilde{x}}^2) \frac{\partial^2}{\partial \tilde{y}^2} + \frac{\partial^2}{\partial \tilde{x}^2} - 2\sigma_{\tilde{x}} \frac{\partial^2}{\partial \tilde{x} \partial \tilde{y}} - \sigma_{\tilde{x} \tilde{x}} \frac{\partial}{\partial \tilde{y}}, \quad (17)$$

and Q , given by (11), becomes

$$Q = \left[(1 + \sigma_{\tilde{x}}^2) \left(\frac{\partial \psi}{\partial \tilde{y}} \right)^2 - 2\sigma_{\tilde{x}} \frac{\partial \psi}{\partial \tilde{x}} \frac{\partial \psi}{\partial \tilde{y}} + \left(\frac{\partial \psi}{\partial \tilde{x}} \right)^2 \right]^{1/2}. \quad (18)$$

Next we introduce the boundary-layer scalings,

$$\hat{x} = \tilde{x}, \quad \hat{y} = \text{Ra}^{1/2} \tilde{y}, \quad \psi = \text{Ra}^{1/2} \hat{\psi}. \quad (19)$$

Thus, on substituting (19) into (14) to (18) and allowing $\text{Ra} \rightarrow \infty$, we obtain the following boundary-layer equations for the present problem,

$$(1 + \sigma_{\hat{x}}^2) \frac{\partial^2 \hat{\psi}}{\partial \hat{y}^2} + \text{Gr}^* (1 + \sigma_{\hat{x}}^2)^{3/2} \frac{\partial}{\partial \hat{y}} \left(\frac{\partial \hat{\psi}}{\partial \hat{y}} \right)^2 = \frac{\partial \theta}{\partial \hat{y}}, \quad (20)$$

$$(1 + \sigma_{\hat{x}}^2) \frac{\partial^2 \theta}{\partial \hat{y}^2} = \frac{\partial \hat{\psi}}{\partial \hat{y}} \frac{\partial \theta}{\partial \hat{x}} - \frac{\partial \hat{\psi}}{\partial \hat{x}} \frac{\partial \theta}{\partial \hat{y}}, \quad (21)$$

these equations are also subject to the boundary conditions (16).

The above equations may be reduced to a form more convenient for numerical solution by means of the further transformation,

$$\xi = \hat{x}, \quad \eta = \frac{\hat{y}}{(1 + \sigma_{\hat{x}}^2) \xi^{1/2}}, \quad \hat{\psi} = \xi^{1/2} f(\xi, \eta). \quad (22)$$

Substituting of (22) into Equations (20) and (21) yields

$$f' + \text{Gr}^* (1 + \sigma_{\xi}^2)^{-(1/2)} (f')^2 = \theta, \quad (23)$$

$$\theta'' + \frac{1}{2} f \theta' = \xi \left(f' \frac{\partial \theta}{\partial \xi} - \theta' \frac{\partial f}{\partial \xi} \right), \quad (24)$$

where it should be noted that (23) has been obtained by integrating once the transformed form of (20). The new boundary conditions are

$$f = 0, \quad \theta = 1 \quad \text{on} \quad \eta = 0, \quad (25a)$$

$$f', \theta \rightarrow 0, \quad \text{as} \quad \eta \rightarrow \infty. \quad (25b)$$

In the above equations primes denote differentiation with respect to η . We note that when $a = 0$ the equations admit self-similar solutions identical with those obtained in [8] and [11]. The solutions are also self-similar when the modified Grashof number, $\text{Gr}^* = 0$; see [4]. When neither parameter is zero, the solutions are not self-similar.

The local Nusselt number is given by

$$\text{Nu} = \frac{\bar{x} q_w}{k_c (T_w - T_\infty)}, \quad (26)$$

where k_c is the effective thermal conductivity of the saturated medium, and q_w is the surface heat flux defined as

$$q_w = -k_c \mathbf{n} \cdot \nabla T. \quad (27)$$

Here,

$$\mathbf{n} = (-\sigma_\xi, 1)/(1 + \sigma_\xi^2)^{1/2} \quad (28)$$

is the unit vector normal to the surface. In terms of nondimensional quantities, we have

$$\text{Nu}/\text{Ra}^{1/2} = -\frac{\xi^{1/2}}{(1 + \sigma_\xi^2)^{1/2}} \theta'(\xi, 0) \quad (29)$$

to leading order.

The total rate of heat transfer between the leading edge and a streamwise location $\bar{x} = \bar{X}$ is given by

$$q_g = \int_0^{\bar{X}} -k(\mathbf{n} \cdot \nabla T)_{\bar{y}=\bar{s}(\bar{x})} \frac{d\bar{s}}{d\bar{x}} d\bar{x}, \quad (30)$$

where \bar{s} is the distance along the wavy surface. In terms of the nondimensional variables this expression becomes

$$q_g = -k(T_w - T_\infty) \text{Ra}^{1/2} \int_0^{\bar{X}} \frac{\theta'(\xi, 0)}{\xi^{1/2}} d\xi. \quad (31)$$

3. Results and Discussion

The results of solving numerically the governing partial differential Equations (23) and (24) subject to the boundary conditions (25) were obtained by using a Keller-box method [13] for a range of values of the parameters a and Gr^* . A total of 131 unevenly spaced points were taken in the η -direction, whilst the constant step in the ξ -direction was 0.01. The Newton–Raphson procedure for iterating to the solution at each streamwise location was deemed to have converged when the maximum pointwise change in successive iterates was less than 10^{-8} .

Numerical solutions are first presented in the form of graphs of the value of $\theta'(\xi, 0)/(1 + \sigma_\xi^2)$, which is proportional to the local rate of heat transfer; see Equation (29). Figure 2 shows the combined effect of varying both the modified Grashof number and the surface wave amplitude. From this figure it is clear that the local rate of heat transfer decreases when either Gr^* or a is increased from zero. When $\text{Gr}^* = 0$, the boundary-layer flow becomes self-similar, and therefore θ' does not vary with ξ . When Gr^* increases from zero the ‘mean’ rate of heat transfer

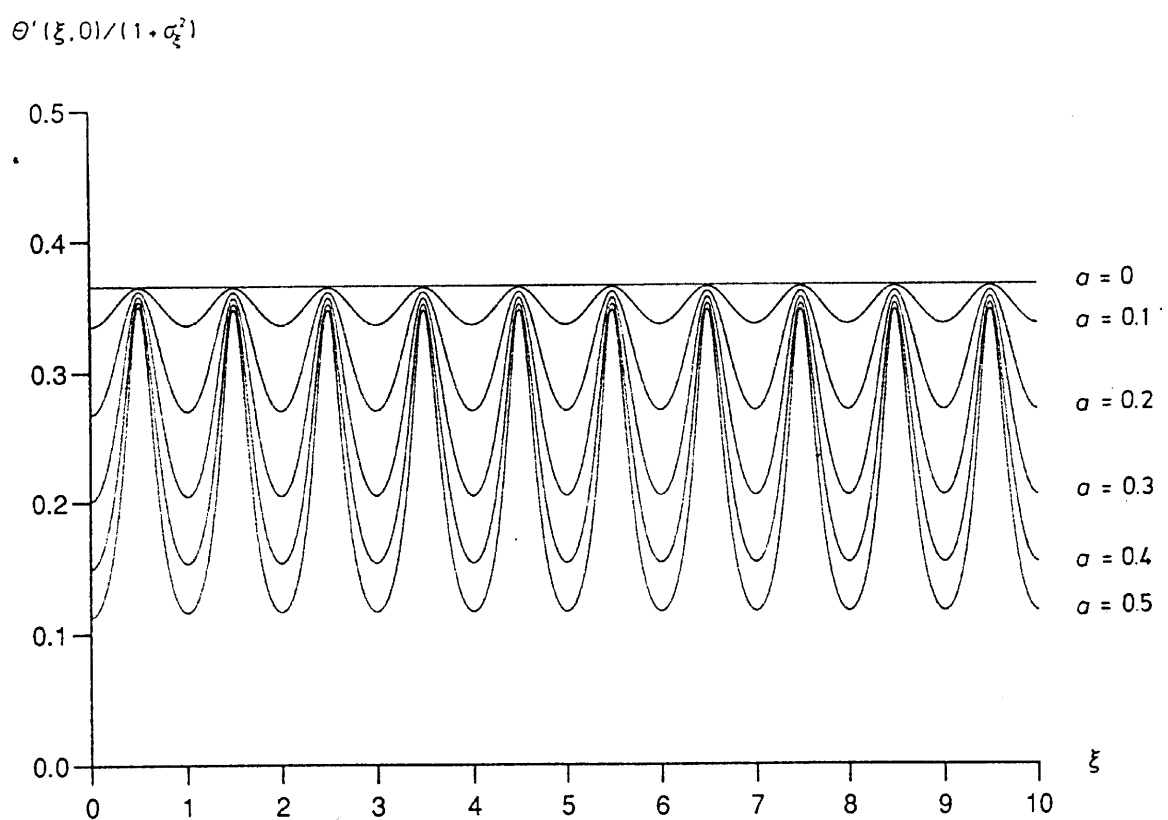
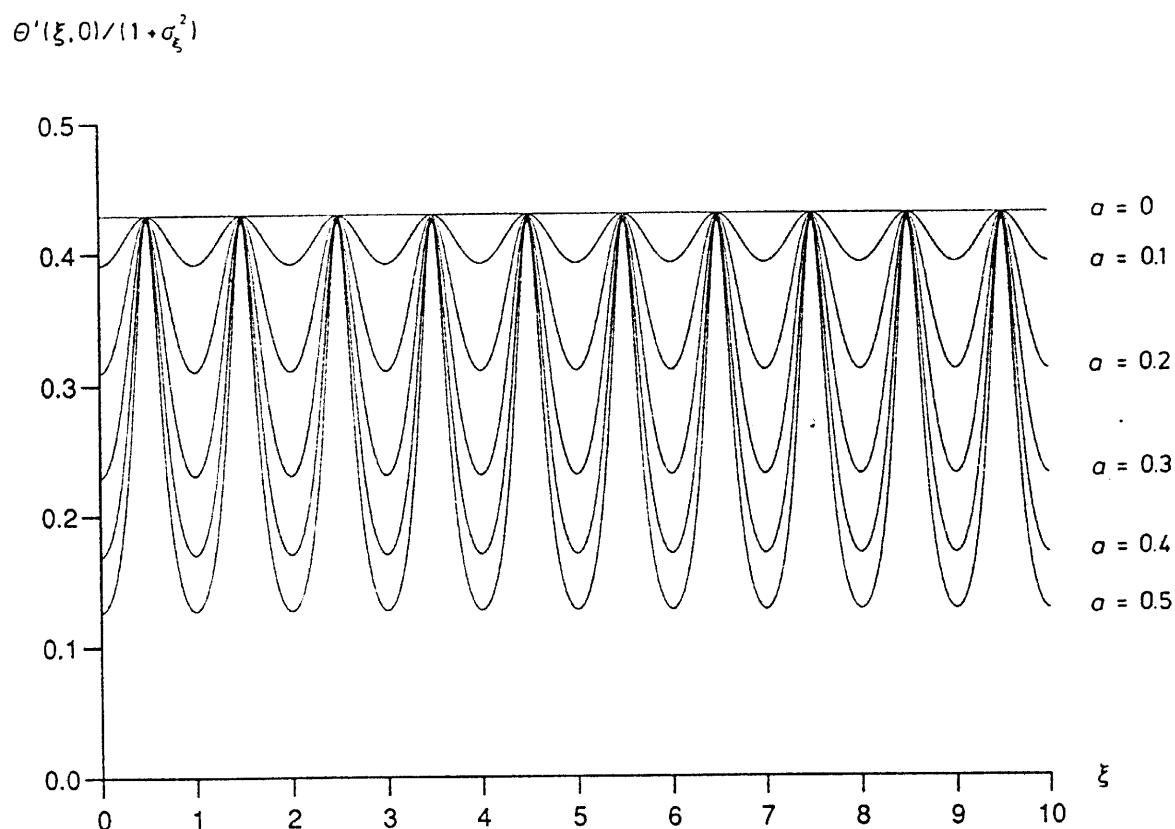


Fig. 2. Variation of the function $\theta'(\xi, 0)/(1 + \sigma_\xi^2)$ for wave amplitudes $a = 0, a = 0.1, a = 0.2, a = 0.3, a = 0.4$ and $a = 0.5$. (a) $\text{Gr}^* = 0.1$, (b) $\text{Gr}^* = 1.0$, (c) $\text{Gr}^* = 10.0$.

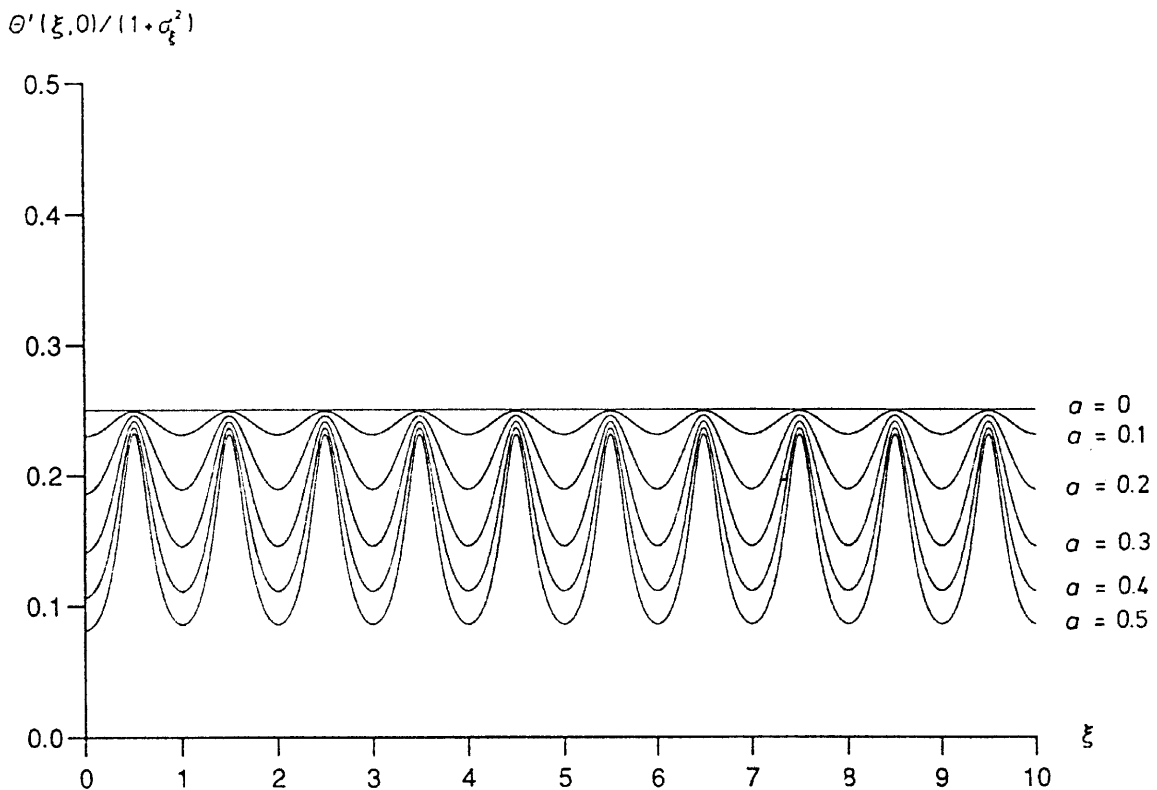


Fig. 2. – (contd.)

from the surface is reduced. This is a consequence of the fact that buoyancy forces are decreasingly able to drive the flow against the fluid inertia. This results in an increased boundary layer thickness, and hence a decreased rate of heat transfer. As in [5], the flow settles down within a few wall wavelengths into a periodic state. Detailed investigations of the full numerical results indicates (i) that no near-wall ‘inner’ boundary layer forms, in contradistinction to the problem considered in [6], where a well-defined sublayer forms as the distance downstream of the leading edge increases, and (ii) that the term, $(f'\theta_\xi - \theta'f_\xi)$, decays to zero as $\xi \rightarrow \infty$ in such a way that the right-hand side of Equation (24) approaches a periodic behaviour with $O(1)$ amplitude. Both these factors rule out a straightforward asymptotic analysis of the solution of (23) and (24) as $\xi \rightarrow \infty$ since all the terms in (24) contribute to the overall balance of magnitudes. Again, when $a = 0$ the boundary-layer flow becomes self-similar, but loses this property otherwise.

Figure 3 shows the effect of varying both parameters on q_g , the global rate of heat transfer given in Equation (30). Although increasing Gr^* decreases q_g , the effect of increasing the wave amplitude, a , is to increase q_g . The strong effect of the presence of surface waves on the *local* rate of heat transfer shown in Figure 2 is now much diminished. This is due to the fact that, when the wavy surface is not vertical, the surface length over which the reduced local rate of heat transfer is integrated is increased. These combined effects nearly cancel each other and the effect of changing a for a fixed value of Gr^* is relatively small.

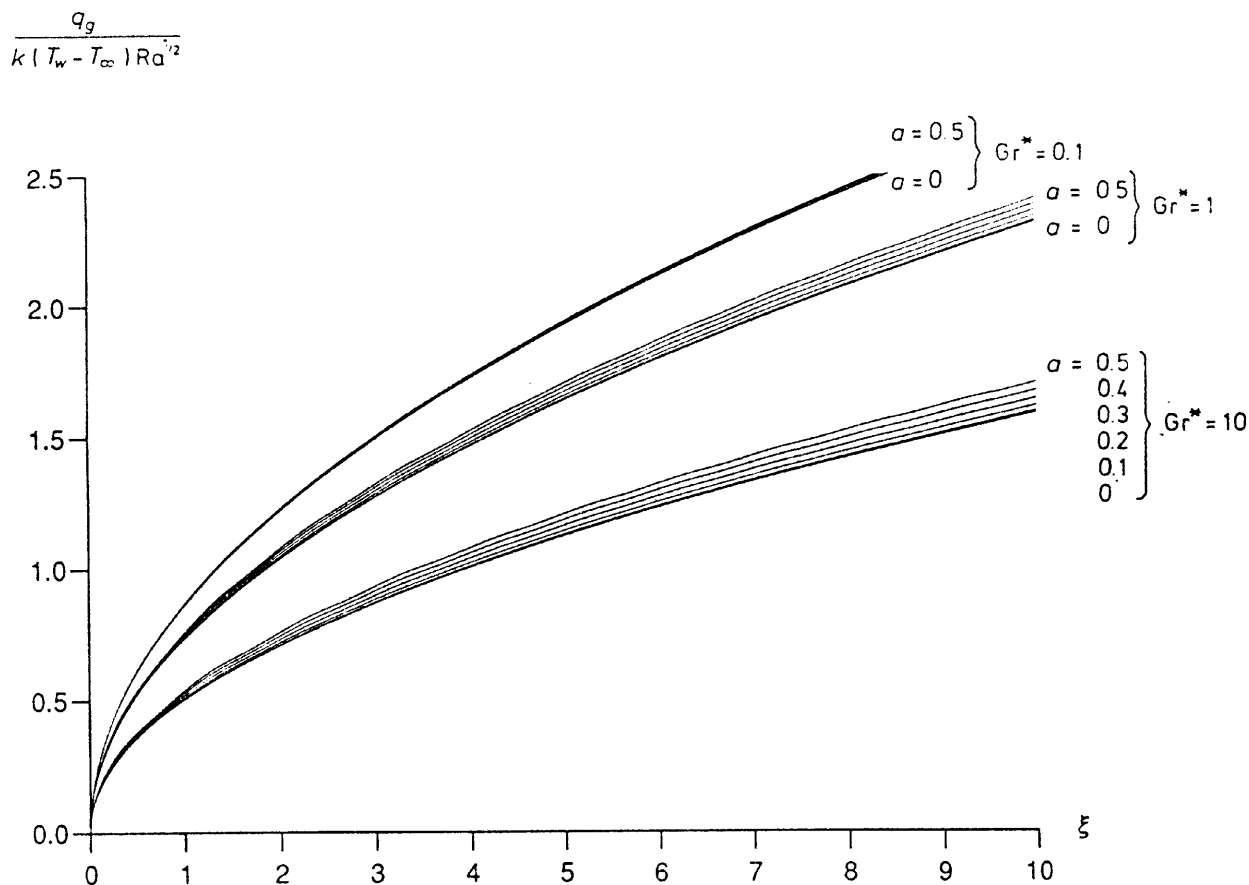


Fig. 3. Variation of $q_g / K(T_w - T_\infty) Ra^{1/2}$ for wave amplitudes $a = 0, a = 0.1, a = 0.2, a = 0.3, a = 0.4$ and $a = 0.5$, and inertia parameters, $Gr^* = 0.1, Gr^* = 1.0$, and $Gr^* = 10.0$.

In conclusion, when the combined effects of surface waves and fluid inertia are taken into account the resulting boundary layer flow induced by a vertical heated surface becomes non-similar. In terms of the local rate of heat transfer from the surface, the presence of waves and fluid inertia serves to decrease the heat transfer. However, in terms of the global rate of heat transfer, the presence of fluid inertia causes a decrease whilst surface waves cause an increase. In the absence of surface waves, inertia decreases the rate of heat transfer, but in the absence of fluid inertia, surface waves do not affect the global heat transfer characteristics (see [4]).

Acknowledgement

The first-named author would like to thank the European Community for providing a Scientist Mobility Scheme Travelling Fellowship which facilitated the research undertaken in this paper.

References

1. Nield, D. A. and Bejan, A.: 1992, *Convection in Porous Media*, Springer, Berlin.
2. Nakayama A. and Koyama, H.: 1987, Free convection heat transfer over a nonisothermal body of arbitrary shape embedded in a fluid-saturated porous medium, *J. Heat Transfer* **109**, 125–130.
3. Nakayama, A. and Koyama, A.: 1987, A general similarity transformation for combined free and forced convection flows within a fluid-saturated porous medium, *J. Heat Transfer* **109**, 1041–1045.
4. Rees, D. A. S. and Pop, I.: 1994, A note on free convection along a vertical wavy surface in a porous medium, *J. Heat Transfer* **116**, 505–508.
5. Rees, D. A. S. and Pop, I.: Free convection induced by a vertical wavy surface with uniform heat flux in a porous medium, *J. Heat Transfer*, in press.
6. Rees, D. A. S. and Pop, I.: Free convection induced by a horizontal wavy surface in a porous medium, *Fluid Dynamics Res.*, in press.
7. Ergun, S.: 1952, Fluid flow through packed columns, *Chem. Engng. Proc.* **48**, 89–94.
8. Plumb, O. A. and Huenefeld, J. C.: 1981, Non-Darcy natural convection from heated surfaces in saturated porous media, *Int. J. Heat Mass Transfer* **24**, 765–768.
9. Vasantha, R., Pop, I. and Nath, G.: 1986, Non-Darcy natural convection over a slender vertical frustum of a cone in a saturated porous medium, *Int. J. Heat Mass Transfer* **29**, 153–156.
10. Lai, F. C. and Kulacki, F. A.: 1987, Non-Darcy convection from horizontal impermeable surfaces in a saturated porous media, *Int. J. Heat Mass Transfer* **30**, 2189–2192.
11. Riley, D. S. and Rees, D. A. S.: 1985, Non-Darcy natural convection from arbitrarily inclined heated surfaces in saturated porous media, *Q. J. Mech. Appl. Math.* **38**, 277–295.
12. Nakayama, A., Koyama, H. and Kuwahara, F.: 1989, Similarity solution for non-Darcy free convection from a nonisothermal curved surface in a fluid-saturated porous medium, *J. Heat Transfer* **111**, 807–811.
13. Keller, H. B. and Cebeci, T.: 1971, Accurate numerical methods for boundary layer flows, 1. Two dimensional flows, in *Proc. Int. Conf. Numerical Methods in Fluid Dynamics*, Lecture Notes in Physics, Springer, New York.